PRACTICAL APPLICATION OF A JACKET-TYPE BREAKWATER WITH A WATER CHAMBER TO THE FISHING PORT

Takayuki Nakamura[1] and Tohru Kouno[2]

.
In this study, a new jacket-type breakwater was proposed for the economical construction of breakwaters in deep-sea ports. This breakwater consists of water chambers with two inclined walls and a submerged horizontal plate. In order to reinforce the breakwater structure, the inclined support piles were adopted instead of vertical piles. Accordingly, the inclined walls were used as front and rear curtain walls. Piston mode wave resonance can be employed in the water chamber to effectively dissipate incoming waves by the generation of separated flows and the resultant vortex flows around the front curtain wall. The performance of the proposed breakwater was examined from the theoretical and experimental viewpoints. Considering the experimental results, we decided to construct an economical water-chamber-type breakwater on the adopted site.

Keywords: water-chamber-type breakwater; seawater exchange; wave transmission: wave reflection

INTRODUCTION

Development of a new jacket-type breakwater with water chambers

The conventional curtain-walled-type breakwater for deep-water conditions and a soft seabed is shown in Fig. 1. It is found that the draft depth of this breakwater increases substantially for regions encountered by sea swells, leading to the generation of a large horizontal wave force. As a result, the design diameter of the support piles becomes large, and thus, uneconomical for construction. Here we propose an economically viable water-chamber-type breakwater, shown Fig. 2 (Nakamura and Yoneshima et al., 2005)

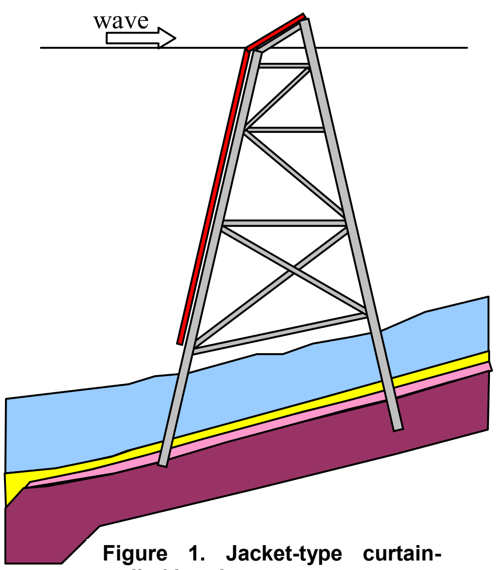

Figure 1. Jacket-type curtain-walled breakwater

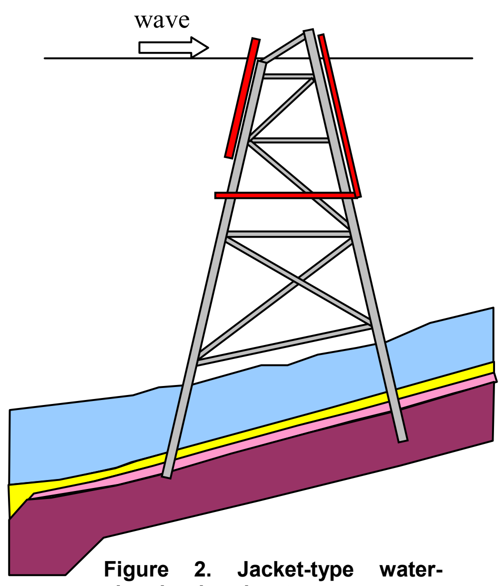

Figure 2. Jacket-type water-chamber breakwater

Previous results

The water-chamber-type breakwater has several advantages (Kouno et al., 2009) such as low reflections, transmissions, and enhanced water exchange performance. We briefly introduce the results of the experiments performed to compare the proposed and the conventional breakwaters. The 1/32 scale models as shown in Figs. 3 and 4 were used in the experiment. The draft depth of the curtain-walled-type breakwater must be comparatively large (97% of the water depth) as compared to that of the water-chamber-type breakwater (37% of the water depth) to keep the calmness in the harbor.

---

[1] Graduate School of Science and Engineering, Civil and Environmental Eng., Ehime University, 3 Bunkyo-cho, Matsuyama 790-0826, Japan
[2] Technological Headquarters, Akiken Civil Engineering Consultancy Inc, 3-25, 4chome Funakoshiminami Aki-ku, Hiroshima 736-0082, Japan

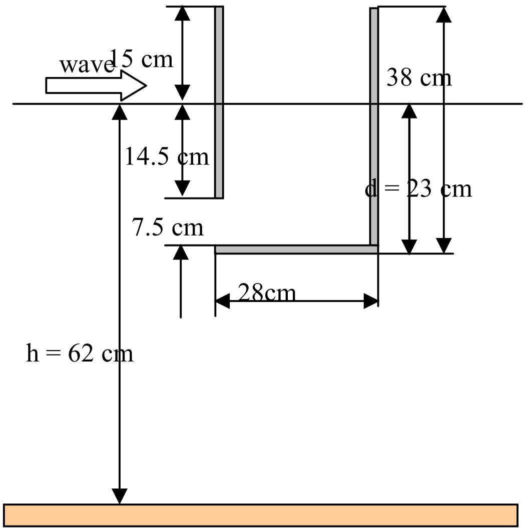

Figure 3. Model of a water-chamber-type breakwater

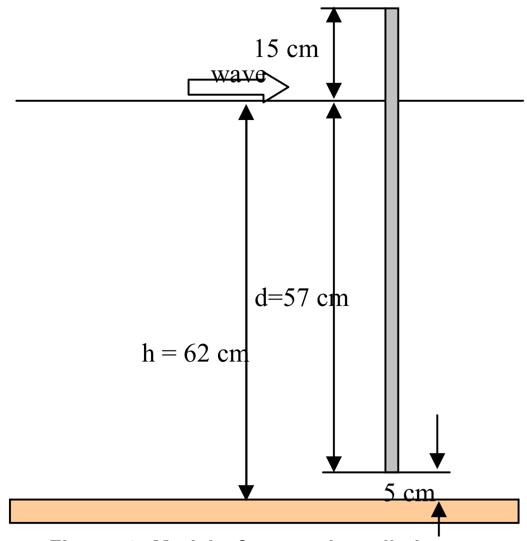

Figure 4. Model of a curtain-walled type breakwater

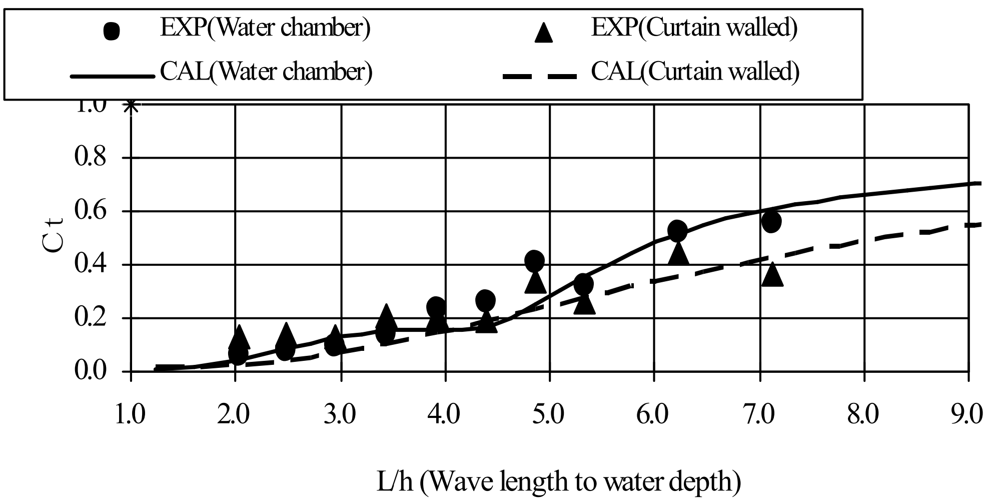

Figure 5. Comparison of the transmission coefficient Ct between the water-chamber-type breakwater and the conventional curtain-walled breakwater

Fig. 5 shows one of typical results of the transmission coefficient Ct of these breakwaters as a function of L/h (wavelength/water depth). From the figure, it can be seen that under the condition L/h = 2 – 5, the transmission coefficient Ct of these two model breakwaters shows very similar tendency with respect to L/h. Therefore, despite a shallower draft, the water-chamber-type breakwater is much more effective to reduce transmitted waves as compared to the curtain-walled-type breakwater with a much deeper draft curtain wall.

Fig. 6 shows a comparison of the reflection coefficient Cr between the curtain-walled-type breakwater and the water-chamber-type breakwater. From this figure, it can be seen that the reflection coefficient Cr of the curtain-walled-type breakwater is much higher than that of the water-chamber-type breakwater. The tendency of higher Cr of the curtain-walled-type breakwater may be attributed to its deeper draft curtain wall.

Fig. 7 shows the result of wave energy dissipation ratio EL for the two breakwater models. Here, EL is defined by Eq. (1),

$$EL = 1 - Ct^2 - Cr^2 \qquad (1)$$

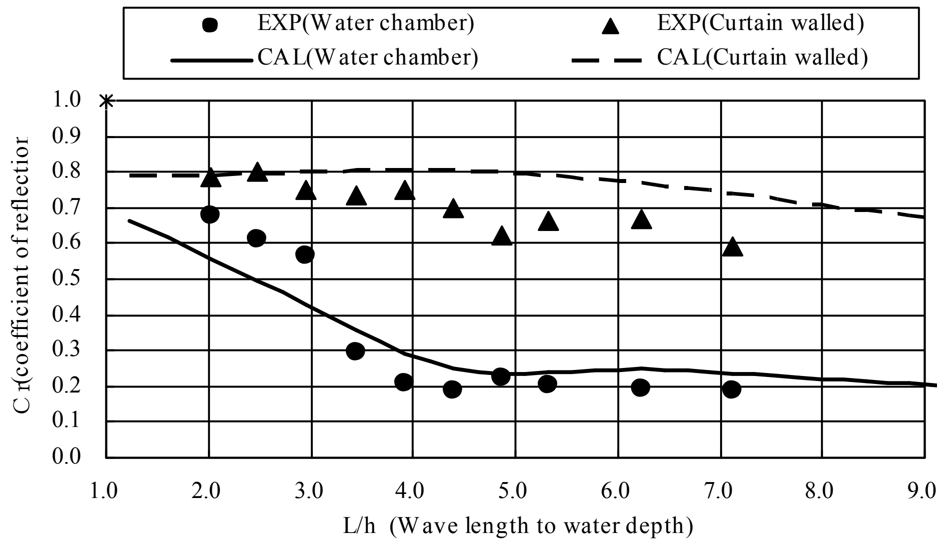

Figure 6. Comparison of reflection coefficient Cr between the water-chamber-type breakwater and the conventional curtain-walled–type breakwater

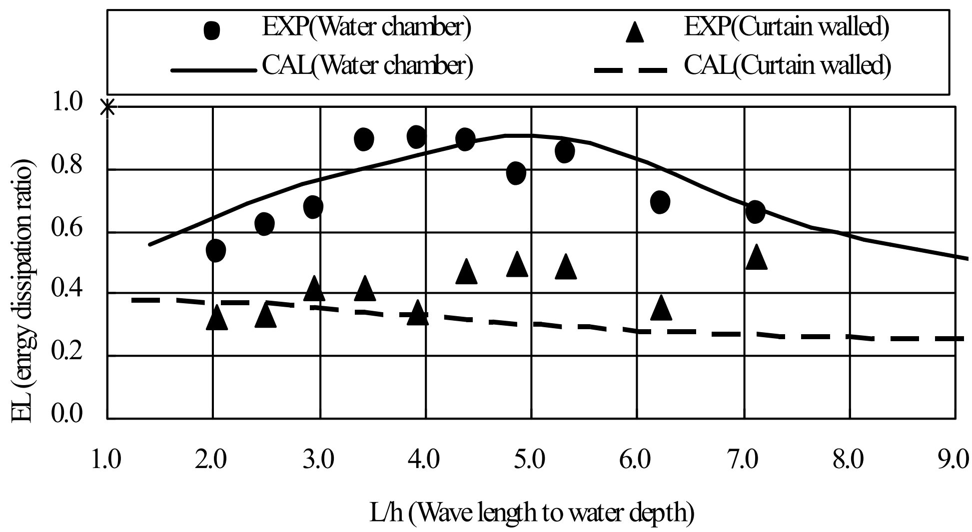

Figure 7. Comparison between EL (energy dissipation ratio) of the water-chamber-type breakwater and the conventional curtain-walled-type breakwater

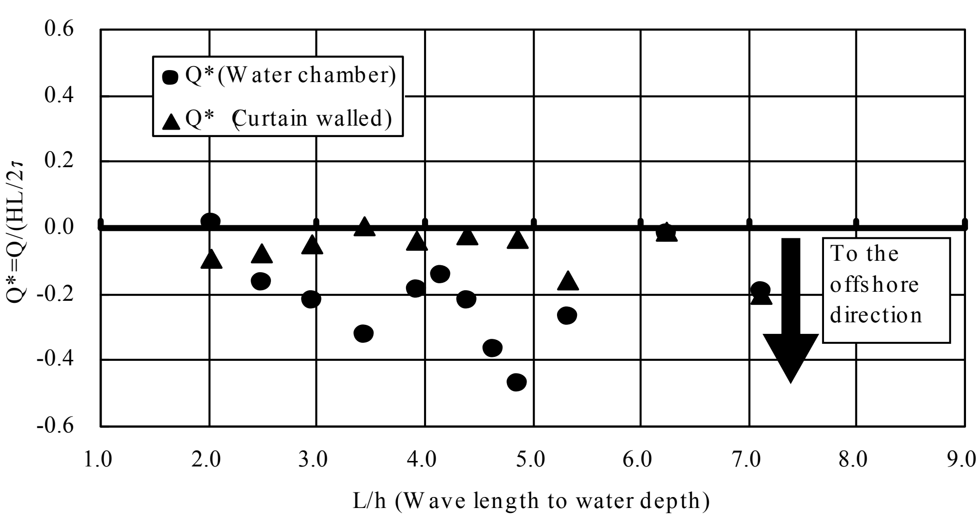

Figure 8. Averaged water mass transport rate for one cycle Q

The difference of wave energy dissipation may be attributed to the fact that in the water-chamber model the vortex flow from the opening under the front wall is strongly excited by the piston mode wave resonance in the water chamber. Furthermore, the difference of the energy dissipation between the two models can also be theoretically predicted by using the damping wave theory (Nakamura and Ide, 1997).

Fig. 8 shows a comparison of the averaged water transport rate during one wave cycle between the two breakwater models as mentioned above. The volume of water transport in one direction Q is normalized by the water mass set in motion during a half wave cycle of sinusoidal wave motions ($=HL/2\pi$).

In Fig. 8, a negative value of Q implies water transport in the offshore direction. In case of the curtain-walled-type breakwater, the opening under the curtain wall is narrow; thus, the average quantity of water transported is small. Additionally, there is no significant driving force for generating the mean current around the curtain-walled-type breakwater.

Practical implementation

We have developed a multi-functional water-chamber-type breakwater, as shown in Fig. 9. Presently, this breakwater is under construction at the location highlighted in Fig. 10, located in Kyushu Island, Japan.

We deemed that the functions of seawater exchange and low transmitted waves were prerequisites for the breakwater design at the port. The proposed breakwater is a pile-supported and jacket-type breakwater with a water chamber of comparatively shallow draft.

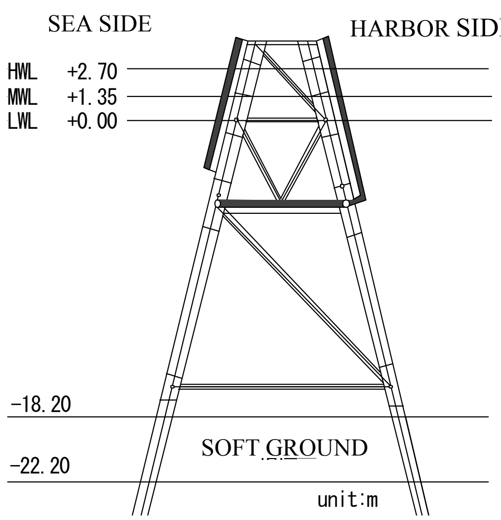

Figure 9. Cross section of the jacket- type water-chamber breakwater

Figure 10. Construction site

Water-chamber-type breakwater

The water depth at the construction site is approximately 20 m at a high water level (HWL) and the seabed is made up of soft soil. Therefore, a pile-supported structure was chosen for the breakwater. In order to enable water exchange in the harbor basin, a water-chamber-type breakwater, as shown in Fig. 9, was adopted after some examinations. Over the past few years, we have proposed and examined a new type of pile-supported breakwater, which, as shown in Fig. 9, has a water chamber close to the surface of the water. It is now known that the water-chamber-type breakwater is effective in reducing transmitted waves as well as reflected waves.

The piston mode wave resonance in the water chamber plays an important role in reducing both the reflected waves and the transmitted waves around the breakwater owing to the generation of large and strong vortices from the lower edge of the front curtain wall. It was also found that the asymmetry of flow separations and the resultant formation of vortices around the front curtain wall for two wave phases, for example, crest and trough, leads to mean water transport in the offshore direction under the base plate of the water chamber. Hence, the proposed breakwater also has a water-exchange function.

We performed two kinds of experiments, i.e. 3-D and 2-D experiments, to verify the water-exchange function of the water-chamber-type breakwater. Only the result of the 2-D experiment will be described in the following.

Wave conditions and required performance

Table 1. Wave conditions and the required performance

Wave conditions	Wave Height H1/3 (m)	Wave Periods T (1/3)	Reflection Coefficient	Transmission Coefficient	Water Exchange
Extreme Waves	2.4	9.4	<0.3	<0.5	-
Critical Waves for Port Access	1	5.3	<0.4	<0.1	Required
Nominal Waves	0.55	5.2	<0.4	<0.1	Required

Tidal Level difference 2.7 m (L.W.L to H.W.L.)

The wave conditions at the construction site are listed in Table 1. The performance prerequisites for each of the target wave conditions are also listed. The cross section of the water-chamber-type breakwater was determined by referring to the previous study (Nakamura et al., 2007).

According to this reference, the characteristic length *la*, which is equal to the square root of the area of the water chamber projected on the front curtain wall, is a very important dimension. When the ratio of a wave length to the characteristic length of the water chamber, L/la, is approximately 10, the minimum wave reflection from the breakwater as well as the maximum wave energy dissipation can be realized. It is also known that for wavelengths $L/la \geq 10$, the significant amount of water is exchanged between the inside and outside harbor because of effective wave interactions with the breakwater.

There were some differences between the previous study and present study, typically in terms of the configuration of the water chamber. In this study, as shown in Fig. 9, we chose a trapezoidal cross section as a water chamber supported by jacket frames. From the point of reinforcement of the breakwater structure, the support piles used should be inclined instead of vertical. In a preliminary study, we have examined the influence of modifying the water chamber cross section on the breakwater performance, typically from the rectangular cross section of water chamber to the trapezoidal one.

EXPERIMENTAL RESULTS

Two-dimensional experiments

We carried out the two-dimensional experiment at Ehime University, using a long-wave flume of length 30 m, height 1.2 m, and width 1 m. Model scale was 1/33.3, and Froude's law of similarity was assumed. Both the regular and the irregular wave conditions corresponding to the conditions at the breakwater construction site were used. Three different tidal levels corresponding to HWL (high water level), MSL (mean sea level), and LWL (low water level) were realized in this experiment.

The following items were measured: 1)Reflection and transmission coefficients, Cr and Ct; 2)horizontal velocity distributions under the base plate and the resultant mass transport velocity in the horizontal direction; and 3)wave pressure distributions among the member plates and the resultant wave forces.

Reflection and transmission coefficients

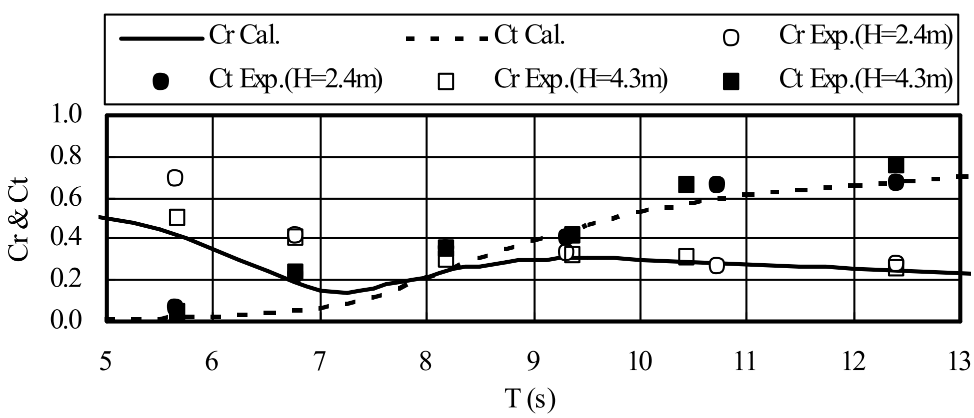

Figure 11. Reflection and transmission coefficients (HWL; regular wave)

Figs. 11 and 12 show the result of Cr and Ct for regular waves at HWL and LWL, respectively. From these figures, it can be seen that the values of Ct for regular waves at HWL and LWL are almost the same; however, the values of Cr at HWL are slightly higher than those at LWL in the case of short wave period conditions.

Figs. 13 and 14 show the result of Cr and Ct of the irregular wave at HWL and LWL, respectively. From these figures, it is also seen that even in the case of irregular wave, under the condition of LWL, the reflection coefficients are higher for short period of waves. The difference between the Cr and the Ct of regular waves and irregular waves at the same water level is not so large as seen in these figures. It can be confirmed that experimental results of Cr and Ct satisfy a required performance of Table 1, regardless of the sea level.

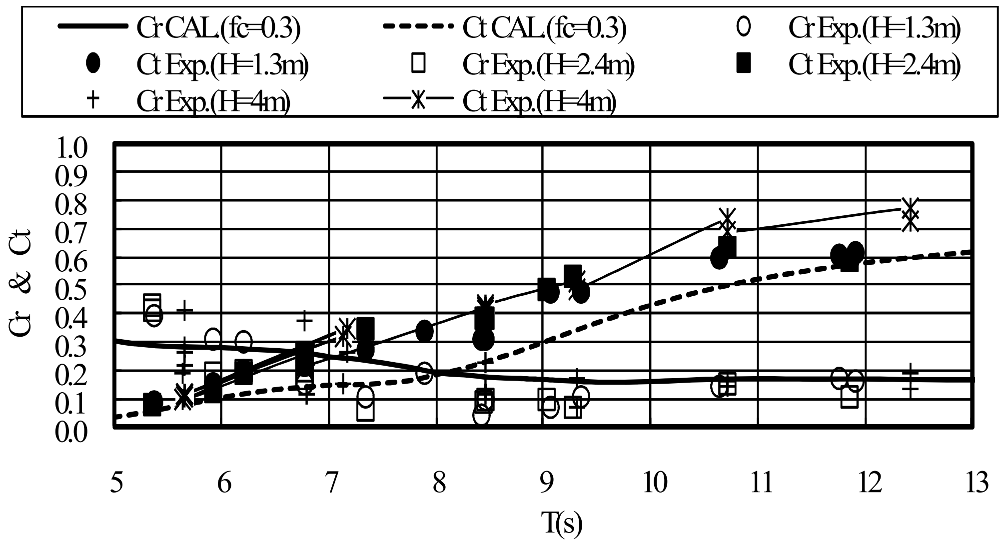

Figure 12. Reflection and transmission coefficients (LWL; regular wave)

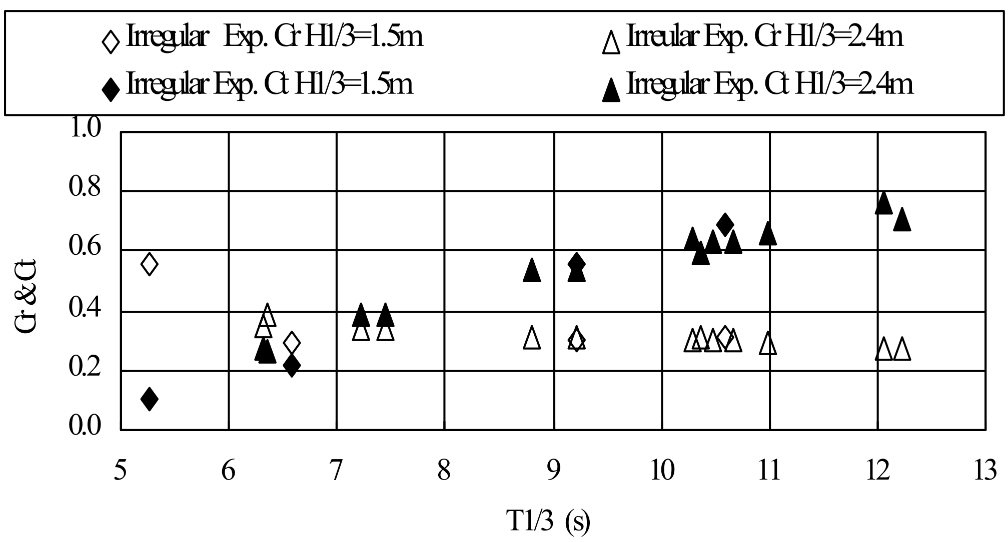

Figure 13. Reflection and transmission coefficients (HWL; irregular wave)

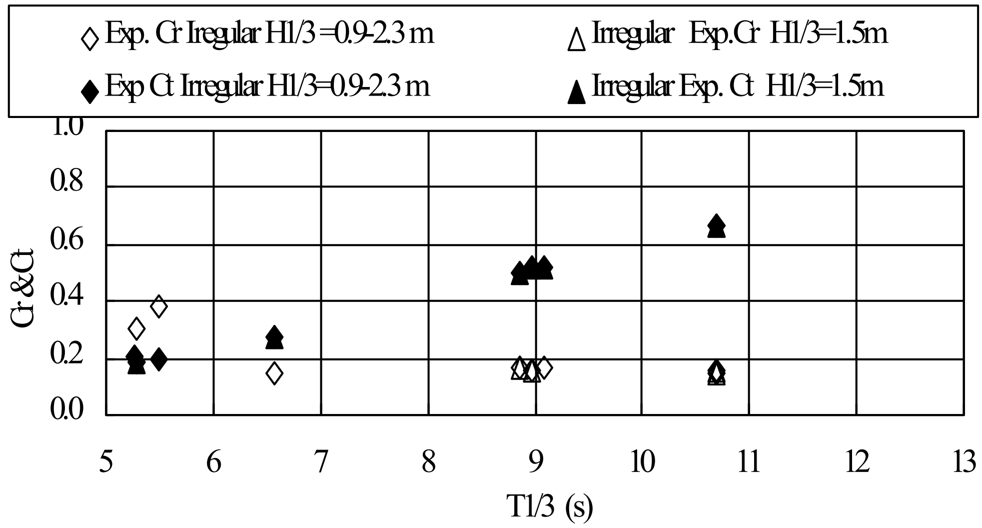

Figure 14. Reflection and transmission coefficients (LWL; irregular wave)

Sea water exchange

Figs. 15 and 16 show the averaged mass transport rate Q* per cycle under the base plate of the breakwater. These figures show that the volume of seawater exchanged under both regular waves and irregular waves under the water level of MSL. The volume of water exchanged of regular wave is larger than that of irregular wave this difference in the volume of water exchanged can be attributed to the irregularities of waves. Besides, the water-chamber-type breakwater has a wide opening under the submerged plate that leads to additional water exchange such as tidal current.

Dimensionless water mass transport rate Q* is approximately 0.15 under nominal wave conditions, and this ratio increases with the wave height and the wave period for an irregular wave. Fig. 15 shows that the rate of water exchange is high for regular waves the rate of water exchange in this case is greater than 0.2 under nominal wave conditions, and it increases with the wave height and the wave period.

It has been also confirmed that the breakwater shown in Fig. 9 is effective for the water exchange under both the LWL and the HWL.

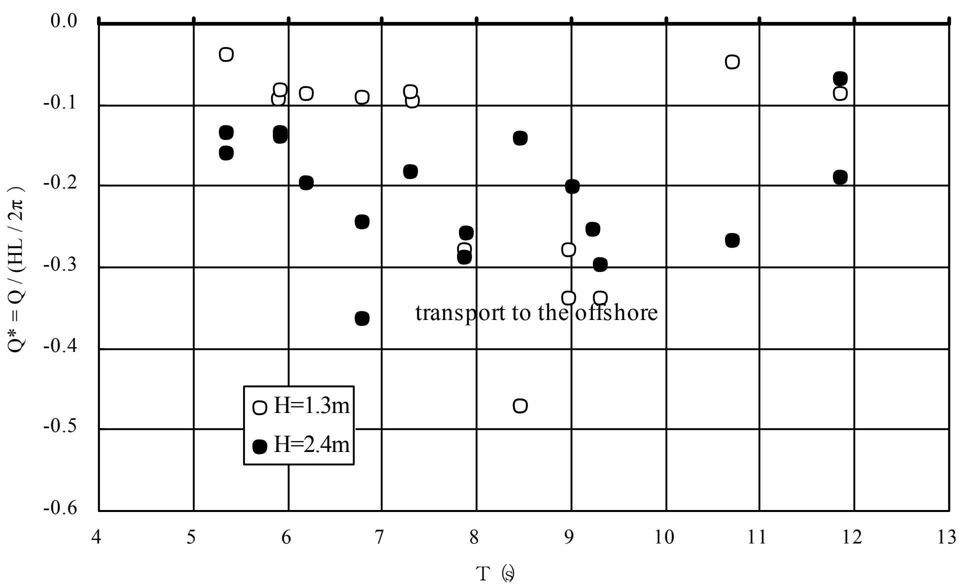

Figure 15 Averaged water transport rate Q (regular waves, MSL)

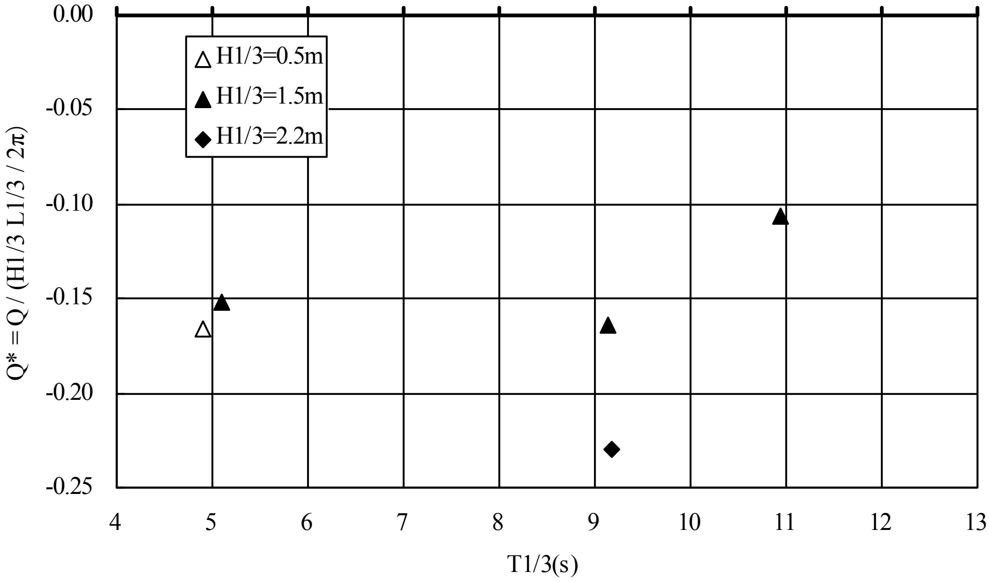

Figure 16. Averaged water transport rate Q （Irregular waves, MSL)

Wave forces

In this section, we describe the result of horizontal wave force Fxi, vertical wave force Fz, and total wave force TFx on the model breakwaters of water-chamber type. For specifying these wave forces, both the positive and the negative peak values of the wave forces are used in their dimensionless forms, which are defined by Eqs. (2) and (3).

$$Fxi^* = Fxi /(w_0 H \; Sf \text{ or } Sb) \; (i=1, 2; \; SF \text{ for } i=1, \; Sb \text{ for } i=2) \qquad (2)$$

$$Fz^* = Fz /(w_0 H \; Bb) \qquad (3)$$

where, w_0: unit weight of fluid; Sf and Sb: draft depth of the front and rear walls, respectively; Bb: width of the horizontal submerged plate; H: incident wave height (for irregular waves, the maximum wave height Hmax is used). The positive direction of wave forces are defined as follows; positive in the wave propagation direction for horizontal wave forces on the front and rear walls as well as on the total body. Positive in the upward direction for the submerged plate in the water chamber.

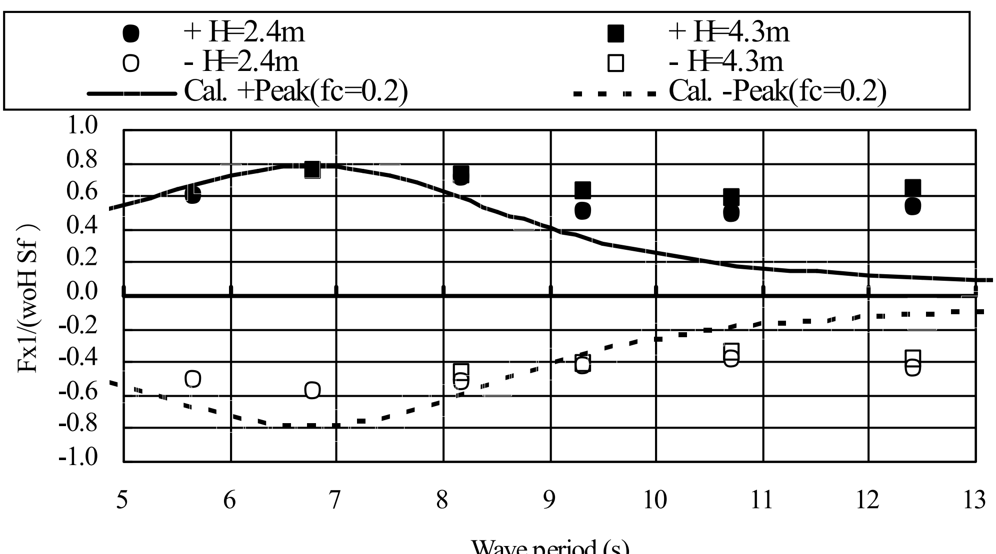

Figure 17. Regular wave force acting on front wall Fx1* (HWL)

The horizontal wave force under HWL is greater than that under LWL; therefore, in the following, we describe the result of horizontal wave forces only at HWL. A comparison between the wave forces acting on the breakwater wall under both the HWL and the LWL conditions reveals that except in the case of the submerged plate, the force acting under the HWL condition is greater than that acting under the LWL condition. The difference between the wave forces acting on the front and rear walls under regular and irregular wave conditions is not considerable. However, in terms of the total wave force, the difference between the force acting under the abovementioned conditions is large (Figs. 25 and 26). This large difference can be attributed to the phase lag of the irregular waves. We accounted for this difference while designing the breakwater.

Figs. 17 and 18 show the results of an experiment performed to determine the intensity of the wave force acting on the front wall of the breakwater, owing to both the regular and the irregular waves. These results indicate that regular and irregular waves have nearly the same intensity on the front wall; however, according to theoretical computation, their intensity decreases with time.

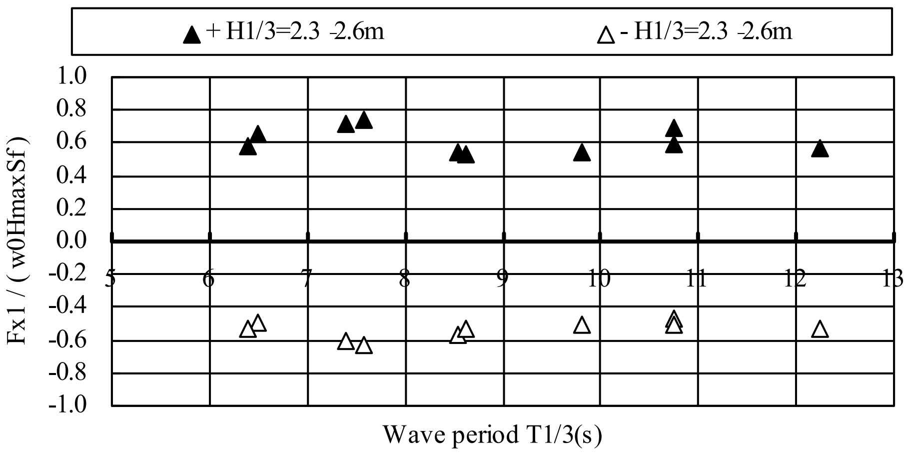

Figure 18. Irregular wave force acting on front wall Fx1* (H1/3=2.3-2.6m HWL)

Figs. 19 and 20 show the results of an experiment performed to determine the intensity of wave force acting on the rear wall of the breakwater, owing to both the regular and the irregular waves. These results indicate that both the regular and the irregular waves have nearly the same intensity on the rear wall; however, in the case of irregular waves, for positive values, the experimental results are slightly greater than those for the negative values.

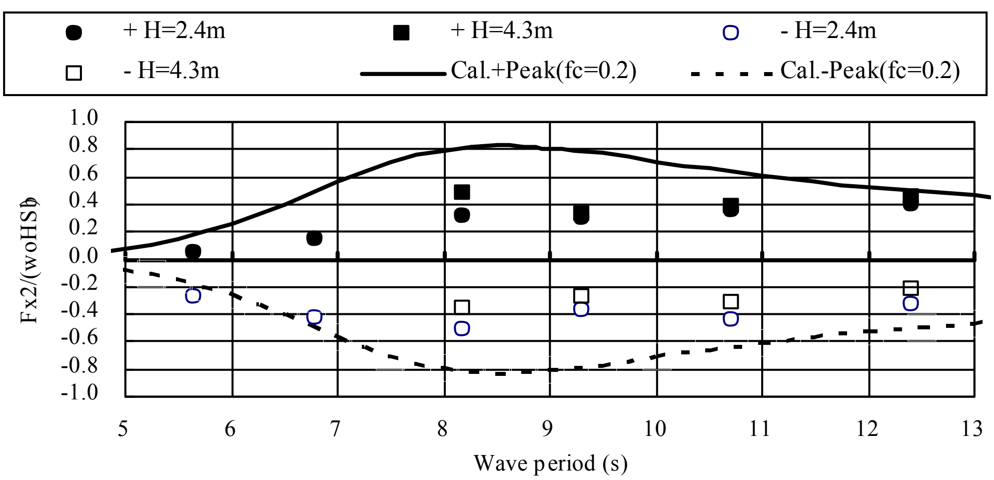

Figure 19. Regular wave force acting on rear wall, Fx2* (HWL)

Figs. 21 and 22 show the results of an experiment performed to determine the intensity of the wave force acting on the submerged plate of the breakwater, owing to both the regular and the irregular waves. These results indicate that both the regular and the irregular waves have nearly the same intensity on the submerged plate.

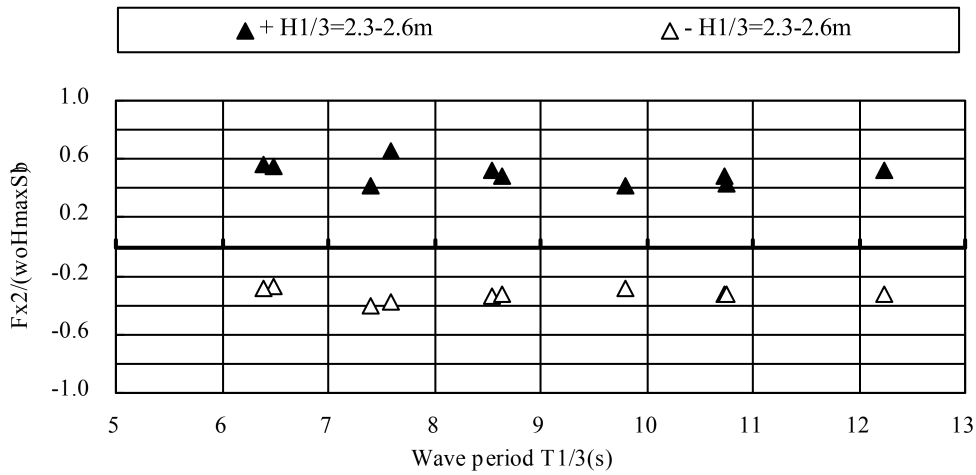

Figure 20. Irregular wave force acting on rear wall, Fx2* (H1/3 = 2.3-2.6 m HWL)

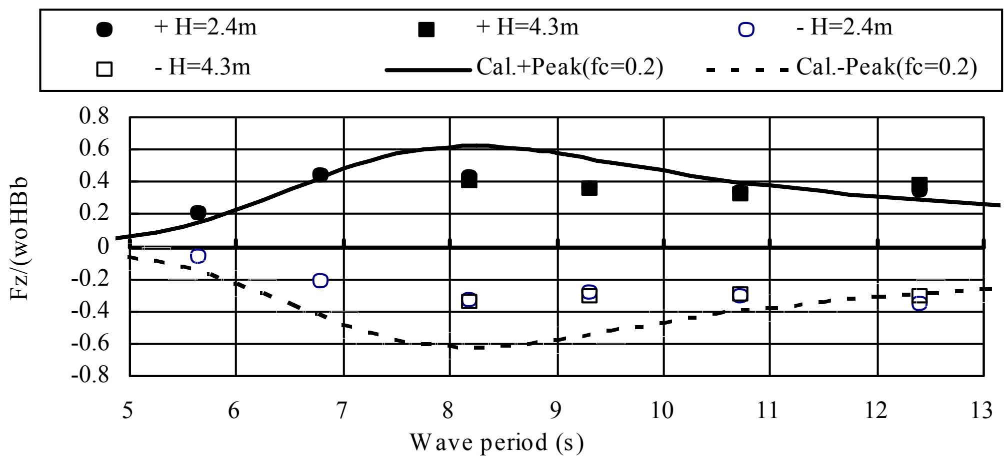

Figure 21. Regular wave force acting on submerged plate, Fz* (HWL)

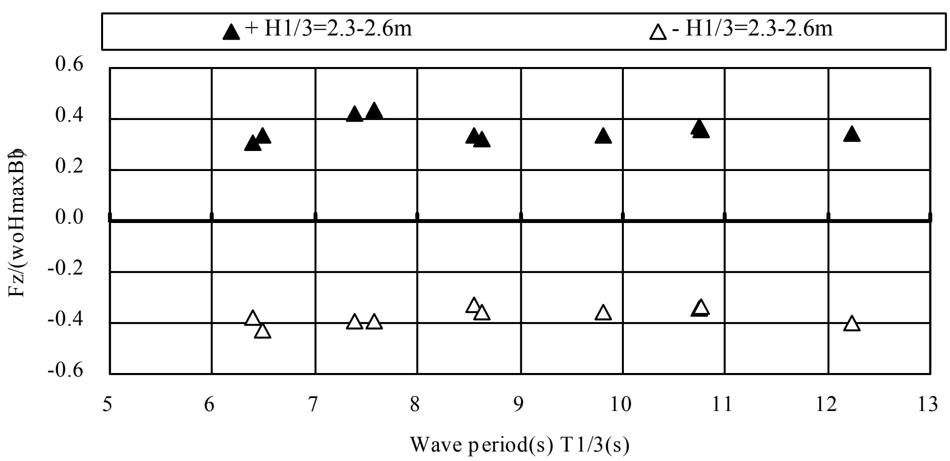

Figure 22. Irregular wave force acting on submerged plate, Fz* (H1/3 = 2.3-2.6 m HWL)

In many cases, the wave force at HWL is large. However, the wave force that acts on the submerged plate owing to a regular wave is large in the case of LWL.

The reason for this large force is clear when we compare Figs. 21 and 23. The difference between the wave forces under HWL and LWL conditions is not considerable for irregular waves, as shown in Figs. 22 and 24.

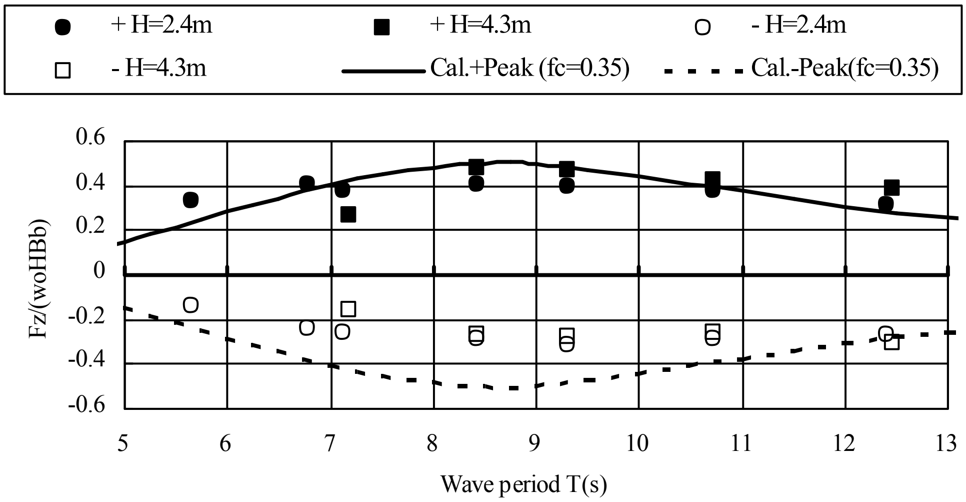

Figure 23. Regular wave force acting on submerged plate, Fz (LWL)

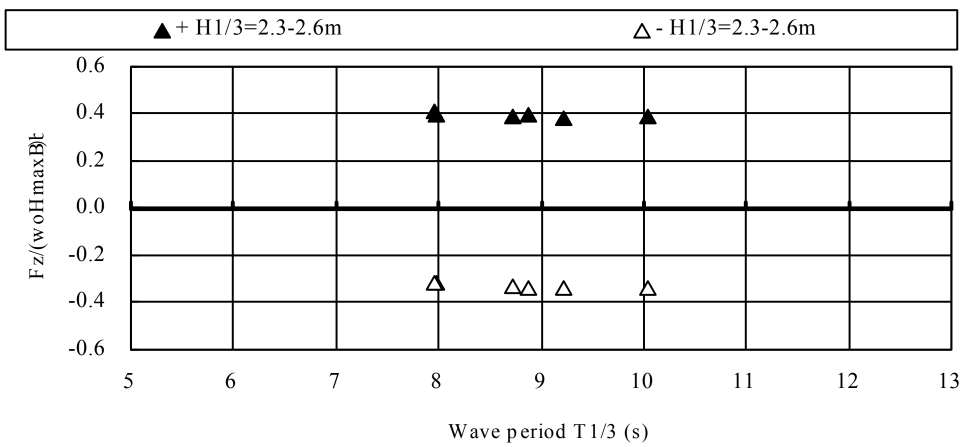

Figure 24. Irregular wave force acting on submerged plate, Fz (H1/3 = 2.3-2.6 m LWL)

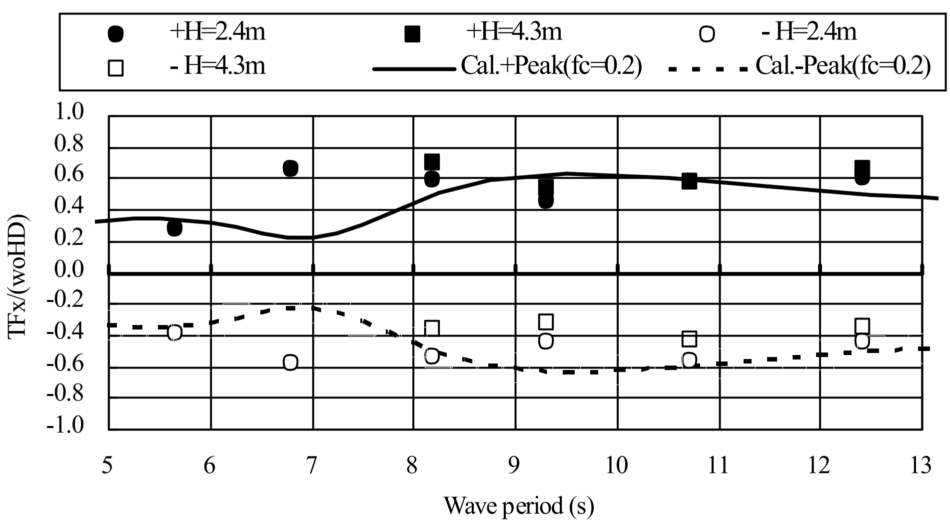

Figure 25. Total horizontal regular wave force TFx* for HWL

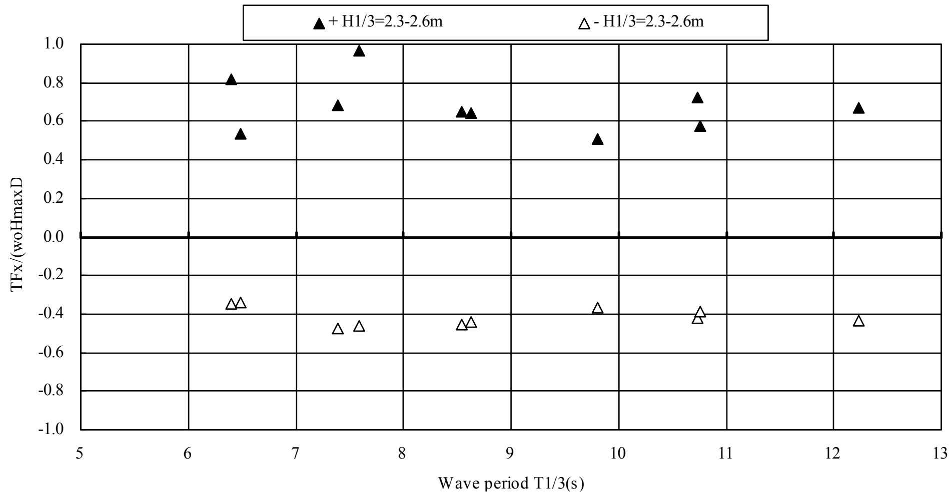

Figure 26. Total horizontal irregular wave force TFx, * (H1/3 = 2.3～2.6 m HWL)

Figs. 25 and 26 show the results of an experiment performed to determine the total wave force acting on the water-chamber-type breakwater under regular and irregular wave conditions. The results indicate that the wave force is larger under irregular wave conditions than under regular wave conditions.

The wave force tends to become large in the experiment; however, it actually decreases in the theoretical calculations for a regular wave in the middle range of wave period.

Phase lags of wave forces

Fig. 27 shows the phase lag of wave forces on each member in regular waves at HWL. The phase lag is measured based on the positive peak of the total horizontal force. Hence the phase lag of 0 degree means in phase relation with the positive peak of the total horizontal force. From this figure, it can be clearly seen that the phase lags among these force components are comparatively large and definite. Using the information shown in this figure, we can easily derive a formula for estimating time variations of the total horizontal force from the member forces on the front and rear walls. Hence the total horizontal wave force considering the phase lag is given by Eq.(4).

$$TFx = Fx1 \times \cos(\omega t - \delta_1) + Fx2 \times \cos(\omega t - \delta_2) \qquad (4)$$

where TFx = Total horizontal wave force; Fx1 = maximum wave force acting on the front wall; Fx2 = maximum wave force acting on the rear wall; ωt = time wave phase; δi(i=1,2) = phase lag of the local wave force acting on the front and the rear wall.

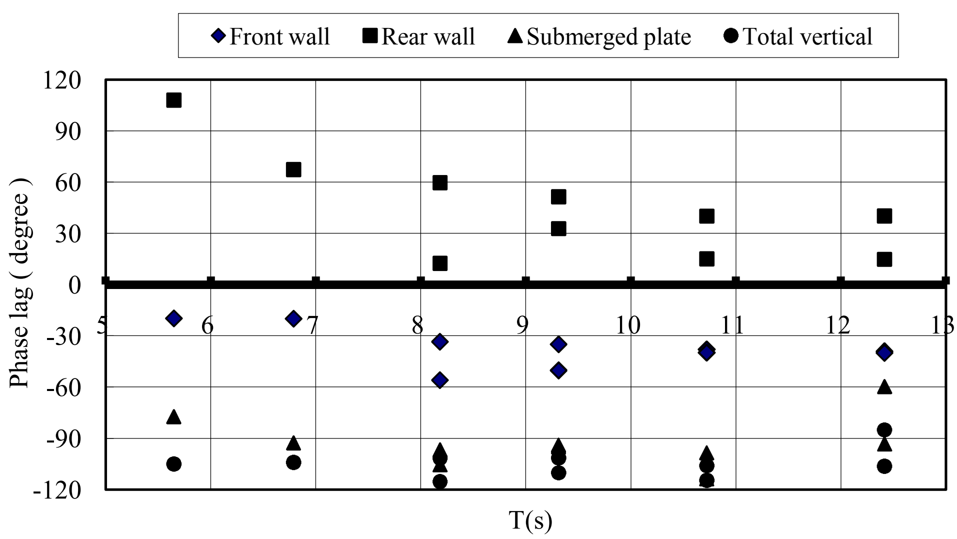

Figure 27. Phase lags among various wave forces acting on the water-chamber-type breakwater (based on the total horizontal force)

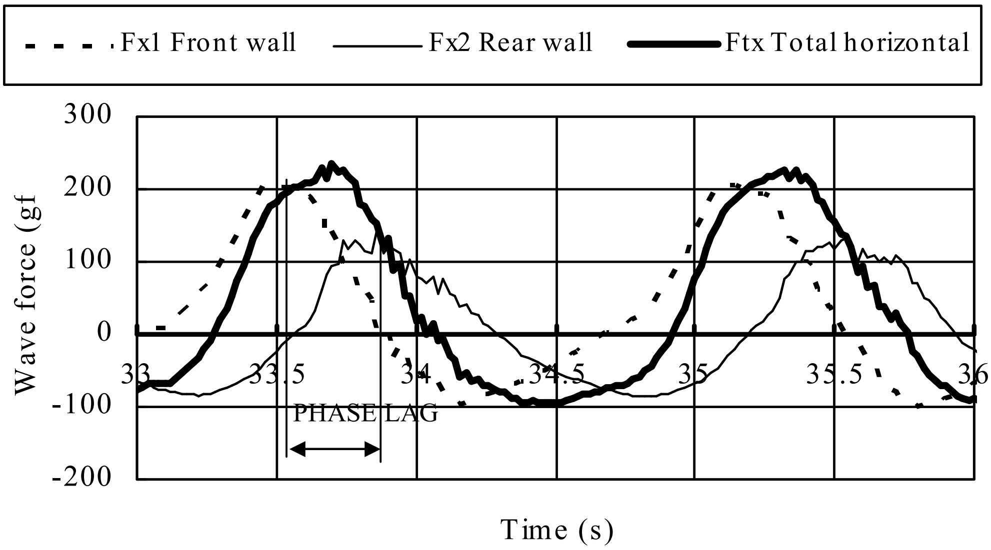

Figure 28. Time-variation curves of the local wave forces and their time-phase relations (HWL; regular wave)

Fig. 28 shows the time-variation curves obtained under regular wave conditions for each wall; the phase lag is clearly seen. On the other hand, it is difficult to derive a formula for the total wave force by considering the phase lag of in case of irregular waves as shown in Figs. 29 and 30.Therefore, to simplify the derivation of the abovementioned formula, we may use the phase lag for the regular wave result.

Figs. 29 and 30 show the time-variation curves of wave force components obtained under irregular wave conditions. In these figures, the phase lag is not clearly defined, therefore, it is difficult to identify the peaks of the respective waves.

Fig. 30 shows the time variation curve of wave forces when the force acting on the rear wall and the total wave force are maximum. Although the wave force acting on the front wall is small, the total wave force is large. It is difficult to determine the exact time of occurrence of the maximum total wave force. For the abovementioned reasons, we may carry out the breakwater design load on the phase lag under regular wave conditions. The phase lag of each wall under regular wave conditions is shown in Fig. 28.

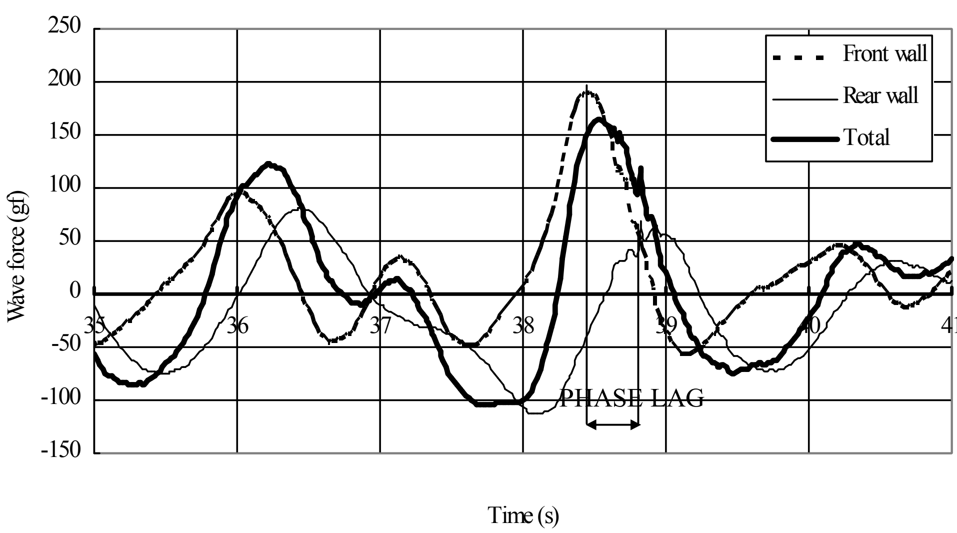

Figure 29. Time-variation curves of local wave forces and their time-phase relations at the front wall max (HWL; irregular wave)

The phase angle between wave forces on the front wall and the rear wall is 40–100°; however, when the wave period becomes longer, the phase angle tends to be smaller. When we compare the total wave force, as shown in Figs. 25 and 26, there is some difference between the forces of the regular wave and the irregular wave.

Ideally, irregular waves represent actual sea conditions, and therefore, they should be used for designing the breakwater. However, it is difficult to derive a formula based on the irregular wave forces. Hence, to simplify the designing process, we can use the formula based on regular wave conditions. However, the value of the maximum wave force was set such that it was greater than that under irregular wave conditions.

On the basis of the total wave force of irregular waves, the phase angle between the front and the rear walls was designed as 60°. In the design of the offshore structure the maximum wave height is adopted instead of the significant wave height typically the maximum wave height is approximately 1.8 times the significant wave height.

The actual calculations were performed for each wall, considering the maximum wave forces acting on each wall under both the LWL and the HWL conditions. We performed design calculations for different 24 times stages. The actual design calculations were performed for each wall, considering the maximum wave forces acting on them. With the exception of the upper horizontal member and the upper diagonal member, we can carry out the design of most of the members of the jacket structure at the phase of the maximum total horizontal wave force.

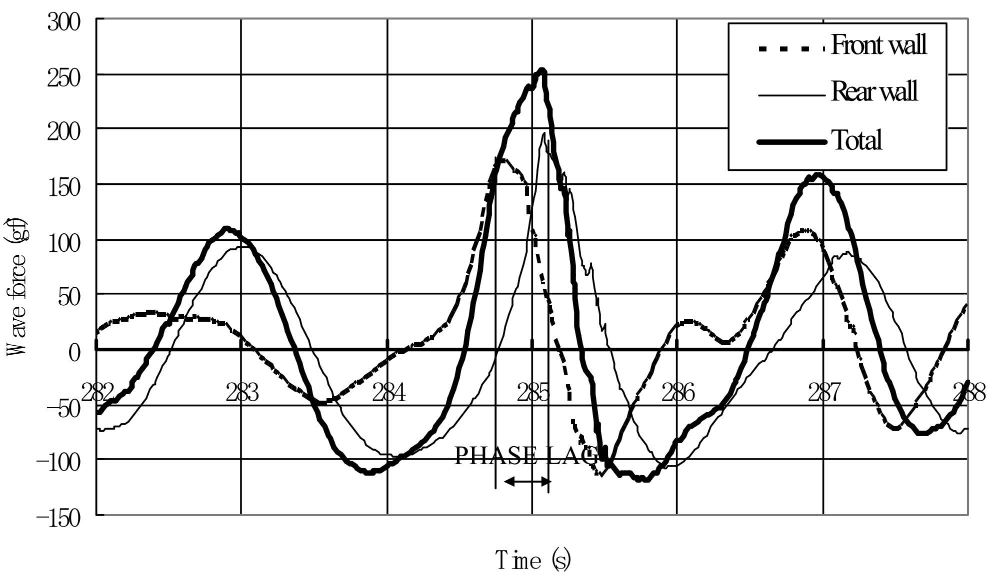

Figure 30. Time-variation curves of the local wave forces and their time-phase relations at the rear wall and total horizontal force max (HWL; irregular wave)

CONCLUSION

Presently, it is possible to predict the wave transmission and reflection coefficients of the newly developed jacket-type breakwater with water chambers; however, it is not possible to accurately estimate the wave force and the amount of seawater exchange of the new breakwater. Then, we have to rely on the laboratory experiment and proceed to the design stage.

From the experimental examination, it was confirmed that the water-chamber-type breakwater supported by jacket frames is very effective for reducing both the reflected and the transmitted waves in deep sea, despite a comparatively shallower draft depth of the water chamber as compared to the water depth. By harnessing wave action, we can use this type of breakwater to facilitate water exchange functions between the harbor and the offshore regions. On the basis of the assumption that the cross-sectional area of the water chamber is approximately same for the both models, i.e. a rectangular and trapezoidal cross section, it was confirmed that the trapezoidal cross section of water chamber is as effective as the rectangular one. The water-chamber-type breakwater supported by jacket frames can be designed such that its draft is shallow; this implies that the wave forces acting on the breakwater are small as compared to those acting on the conventional curtain-walled-type or gravity-type breakwaters.

. We intend to carry out a field observation after the completion of breakwater construction to verify the experimental results. In this field observation, we will plan to measure the transmission and reflection coefficients and the volume of water exchange.

ACKNOWLEDGEMENT

The authors wish to thank the Nagasaki Prefecture Office and JIFIC (Japanese Institute of Technology on Fishing Ports, Grounds and Communities) for supporting this study.

REFERENCES

Kouno, T. & Nakamura, T. 2009 Jacket-type Breakwaters with Water Chambers in Deep Sea, *2009 Annual ISOPE- vol. 3 pp. 1010-1016.*

Nakamura, T. & Ide, Y. 1997 Analysis on wave transformations and wave force about an angular body considering wave energy dissipations, *Proc. of Civil Eng. in the Ocean, vol. 13, pp. 177-182 (in Japanese).*

Nakamura, T., Yoneshima, M., & Tanaka, K. 2005 Effectiveness of a jacket-type breakwater with water chamber for comparatively long waves in deep sea ports, *Proc. of Coastal Engineering, vol. 52, pp. 671-675 (in Japanese).*